

Single-Photon Generation

Nuno A. Silva^{*†}, Nelson J. Muga^{*†}, and Armando N. Pinto^{*‡}

^{*}Instituto de Telecomunicações, Aveiro, Portugal

[†]Departamento de Física, Universidade de Aveiro, Portugal

[‡]Departamento de Electrónica, Telecomunicações e Informática, Universidade de Aveiro, Portugal

Emails: nasilva@av.it.pt, muga@av.it.pt, and anp@ua.pt

Abstract—We analyse experimentally and theoretically the generation of single-photons through four-wave mixing process in optical fibers in a low power regime. The coupled-equations for the electrical field complex amplitudes are derived and solved. The proposed model is compared with experimental data. We show the importance of the nonlinear contribution to the phase-matching condition and the influence of the polarization effects on the generation of the single-photons. The 8/9 factor for the nonlinear coefficient is confirmed by direct measurement of the number of photons on the idler wave.

I. INTRODUCTION

The dependence of the fiber index of refraction on the applied electrical field, Kerr effect, gives rise to an intensity-dependent phase shift of the optical field. Four-wave mixing (FWM) is a Kerr nonlinear process in optical fibers. This nonlinear process is governed by the third-order nonlinear susceptibility $\chi^{(3)}$ [1]. In the FWM process no energy between the optical fields and the fiber is transfer and in that sense the FWM can be considered a elastic process [1]. FWM occurs when light of two or more different optical frequencies are launched into a fiber, given rise to a new frequency. Typically the frequencies launched into the fiber are known as pump and signal fields, and the frequency generated through FWM is known as idler field. At the same time that the idler field is created, the signal wave is amplified [1].

In 1974, the phase-matched nonlinear mixing in a silica fiber was observed [2]. Since then, most of the work related with the FWM process have been done around the zero-dispersion of the fiber, in order to obtain efficient FWM. These experiments were performed in a high power regime in order to enhance the FWM process [3], [4].

Most of the quantum communications protocols requires single or entangled qubits to transmit information between distant locations [5]. Recently, single and entangled photon pairs have been used in quantum key distribution experiments in fiber optics, in order to implement these quantum communications protocols [6], [7].

The FWM process in optical fibers provides a natural way to generate single and entangled photons directly inside a fiber.

In this experiments, the FWM process is obtained in a very low power regime [1].

In this paper we study theoretically and experimentally the FWM process in optical fibers in a low power regime.

This paper contain four sections. In section II, the experimental setup used to analyse the generation of the idler wave through FWM process in a low power regime is described. In section III we present a new theoretical model to describe the FWM process. We discuss the influence of the nonlinear and polarization dependent effects in the efficiency of the FWM process. In section IV the main results of this paper are summarized.

II. EXPERIMENTAL RESULTS

In Fig. 1 we present a schematic of our experimental setup. This setup was used to analyze the average number of photons per pulse and optical power of the idler wave generated through the FWM process in a low power regime.

In the experimental setup, Fig. 1, the pump in continuous mode with wavelength λ_1 passes through a polarization controller (PC), before being coupled to another optical signal λ_2 from a tunable laser source. The signal λ_2 is modulated externally to produce optical pulses with a width at half maximum of approximately 1.6 ns and a repetition rate of 610 kHz. At the

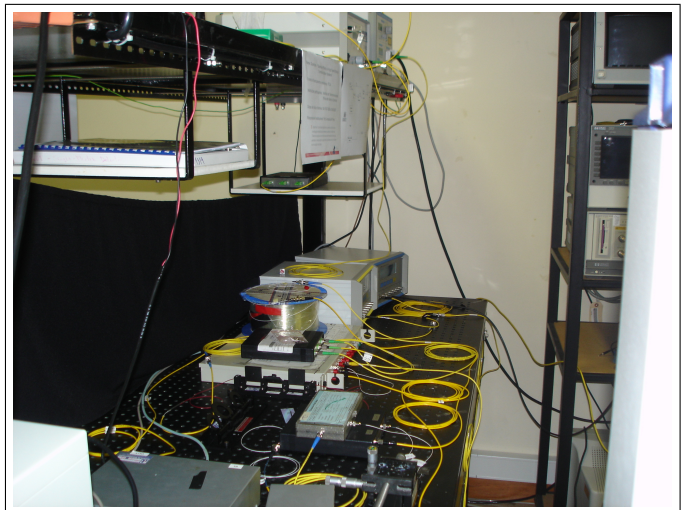


Fig. 1. Experimental setup for measuring the average number of photons per pulse and the optical power generated through FWM in optical fibers in a low power regime. Details of the experimental setup are present in the text.

This work was partially supported by the Institute of Telecommunications under the Associated Laboratorial program supported by the Portuguese Scientific Foundation, FCT, and European Union FEDER program, through the IT/LA projects: “Quantum - Quantum Effects in High Speed Optical Communication Systems” & “QuantTel - Quantum Secure Telecommunications”.

TABLE I
AVERAGE NUMBER OF IDLER PHOTONS PER PULSE VERSUS SPECTRAL SPACING BETWEEN PUMP AND SIGNAL FIELDS

$\lambda_1 - \lambda_2$ nm	\bar{n}	$\lambda_1 - \lambda_2$ nm	\bar{n}
1.251	3.034	5.626	0.821
1.65	3.016	6.022	0.559
2.049	2.959	6.418	0.320
2.447	2.894	6.814	0.164
2.845	2.673	7.210	0.064
3.243	2.525	7.606	0.025
3.640	2.308	8.001	0.051
4.038	2.071	8.397	0.102
4.435	1.778	8.792	0.107
4.832	1.401	9.186	0.115
5.229	1.142	9.581	0.009

modulator output the signal passes from an attenuator which allow us obtain a very low power at the input of the fiber. The two optical fields are launched into a dispersion shift fiber (DSF), with incident powers $P_1(0)$ and $P_2(0)$. The DSF has zero-dispersion wavelength at $\lambda_0 = 1547.34$ nm, length $L = 8865$ m, nonlinear coefficient $\gamma = 2.36 \text{ W}^{-1}\text{km}^{-1}$, attenuation, at λ_0 , $\alpha = 0.2 \text{ dB/km}$ and dispersion slope $dD_c/d\lambda = 0.069 \text{ ps}/(\text{nm}^2\text{km})$. Due to the FWM process a new wave, $\lambda_3 = \lambda_1\lambda_2/(2\lambda_2 - \lambda_1)$ is generated inside the optical fiber. At the fiber output a optical filter eliminates the pump and signal waves, while the idler wave, λ_3 , passes through the filter and reaches a single photon detector. The single photon detector is based on an APD, operating in the so-called Geiger mode, being $T_g = 2.5$ ns the time during in which the gate of the detector is open. The detector quantum efficiency is $\eta = 10\%$ and the dark count probabilities per gate is $Pr_{dc} = 5 \times 10^{-5}$ [8]. The average number of idler photons per pulse that reaches to the single photon detector is given by [8]

$$\langle n \rangle = \frac{1}{\eta} \ln \left(\frac{Pr_{dc} - 1}{Pr_{av} - 1} \right), \quad (1)$$

where Pr_{av} is the probability of avalanche per gate. In Table I we present the average number of photons per pulse given by (1) and the spectral spacing between pump and signal fields, for $\lambda_1 = 1547.57$ nm, $P_1(0) = 8.71$ mW and $P_2(0) = 1.26 \times 10^{-4}$ mW. From Table I we can see that the average number of photons generated per pulse inside the fiber depends of the wavelength separation between pump and signal fields. This mean that with the proposed experimental setup, Fig. 1, we built a photon source which has the advantage of generate a variable average number of photons on the idler wave, by simple adjust of the wavelength separation between pump and signal fields.

The average number of photons that arrive to the single photon detector and the optical power of the idler field at the exit of the fiber are given by

$$\langle n \rangle = P_3 \frac{\lambda_3 T_g}{hc} 10^{-\alpha_d/10}, \quad (2)$$

where P_3 represents the idler power at the exit of the fiber, h is the Planck constant, c is the speed of light in vacuum and $\alpha_d \approx 13$ is the attenuation, in decibels, from the fiber output to the detector.

III. THEORETICAL DESCRIPTION

The FWM process was studied both theoretically and experimentally by Hill *et al.* [9], and their work was latter reformulated by Shibata *et al.* [10]. According with [3], [10] the optical power of the idler wave is given by

$$P_3(z) = (\gamma P_1(0) z_{eff})^2 P_2(0) \exp\{-\alpha z\}, \quad (3)$$

with

$$z_{eff} = \frac{1 - \exp\{-\alpha z\}}{\alpha}, \quad (4)$$

where η is the efficiency of the process given by

$$\eta = \frac{\alpha^2}{\alpha^2 + (\Delta\beta)^2} \left(1 + \frac{4 \exp\{-\alpha z\} \sin^2(\Delta\beta z/2)}{(1 - \exp\{-\alpha z\})^2} \right), \quad (5)$$

and $\Delta\beta$ is the phase-matching condition

$$\Delta\beta = - \frac{2\pi c \lambda_0^3}{\lambda_1^3 \lambda_2^2} \frac{dD_c}{d\lambda} \Big|_{\lambda_0} (\lambda_1 - \lambda_0)(\lambda_1 - \lambda_2)^2. \quad (6)$$

In Fig. 2 we plot the average number of photons per pulse versus theoretical prediction (3), for the idler wave as a function of wavelength separation between pump and signal fields. From Fig. 2 we can see that this model does not describ correctly the experimental results for $\lambda_1 - \lambda_2 > 2.8$ nm, in the low power regime.

A. Nonlinear contribution

In order to improve the theoretical model we present in this section a description of the FWM process. We assume that all fields in the fiber (pump, signal and idler fields) remain co-polarized along the propagation in the fiber,

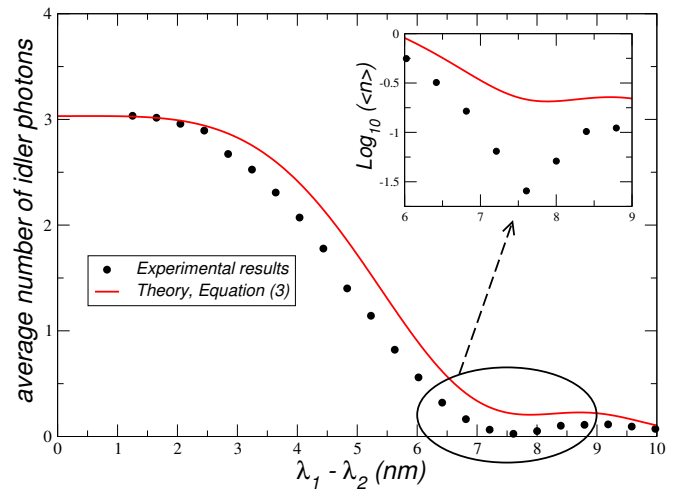


Fig. 2. Average number of photons per pulse generated through FWM process versus theoretical prediction (3), for the idler wave as a function of wavelength separation between pump and signal fields. We have used: $P_1(0) = 8.71$ mW, $P_2(0) = 1.26 \times 10^{-4}$ mW and $\lambda_1 = 1547.57$ nm.

and in order to avoid multiple FWM processes in the optical fiber [11], the fields are maintained in a low power regime. The propagation of the electrical field complex amplitudes inside an optical fiber are governed by the nonlinear Schrödinger equation (NLSE). Under the slowly varying envelope approximation the NLSE is written as [1]

$$\frac{\partial A}{\partial z} + \frac{\alpha}{2}A = \sum_{m=0}^{+\infty} \frac{i^{m+1}\beta_m}{m!} \frac{\partial^m A}{\partial t^m} + i\gamma \left[1 + \frac{i}{\omega_0} \frac{\partial}{\partial t} \right] P^{NL}(z, t), \quad (7)$$

where β_m is the m^{th} order dispersion coefficient and $P^{NL}(z, t)$ is the third-order nonlinear polarization given by

$$P^{NL}(z, t) = A(z, t) \int_0^{+\infty} R(\tau) |A(z, t - \tau)|^2 d\tau, \quad (8)$$

where $R(\tau)$ is the fiber nonlinear response function [1].

Assuming that each field is not dependent of the time, and neglecting the pump depletion we obtain for the pump field [1]

$$A_1(z) = A_1(0) \exp\{i\gamma P_1(0)z_{eff}\} \exp\{-\alpha z/2\}, \quad (9)$$

where $P_1(0) = |A_1(0)|^2$ is the incident power. The evolution of the signal and idler fields is given by [12]

$$\frac{\partial A_2(z)}{\partial z} \approx i \left[\frac{\Delta\beta}{2} + \gamma P_1(z) \right] A_2(z) + i\gamma A_1^2(0) A_3^*(z) e^{-\alpha z}, \quad (10a)$$

$$\frac{\partial A_3(z)}{\partial z} \approx i \left[\frac{\Delta\beta}{2} + \gamma P_1(z) \right] A_3(z) + i\gamma A_1^2(0) A_2^*(z) e^{-\alpha z}. \quad (10b)$$

Assuming that only the pump and the signal waves are launched into the fiber, the optical power of the idler wave at a distance z for $\alpha = 0$ are given by

$$P_3(z) = (\gamma P_1(0)z)^2 P_2(0) \left| \frac{\sinh(\kappa z)}{\kappa z} \right|^2, \quad (11)$$

where κ is the parametric gain given by

$$\kappa = \sqrt{\frac{\Delta\beta}{2} \left(\frac{\Delta\beta}{2} + 2\gamma P_1(0) \right)}. \quad (12)$$

The effect of fiber loss is taken into account by replacing $P_1(0)$ in (11) with $P_1(0)z_{eff}/z$, valid for low-loss fibers [12]. In this approximation the parametric gain is written as

$$\kappa = \sqrt{\frac{\Delta\beta}{2} \left(\frac{\Delta\beta}{2} + 2\gamma P_1(0)z_{eff}/z \right)}, \quad (13)$$

and the optical power of the idler wave can be express as

$$P_3(z) = (\gamma P_1(0)z_{eff})^2 P_2(0) \left| \frac{\sin(\kappa z)}{\kappa z} \right|^2 \exp\{-\alpha z\}. \quad (14)$$

Comparing (3) with (14), the efficiency of the FWM process is now given by $\eta = |\sin(\kappa z)/\kappa z|^2$ and it is dependent of the nonlinear contribution $\gamma P_1(0)$.

In Fig. 3 we plot the measured optical power and the theoretical predictions given by equation (3) and (14) for the

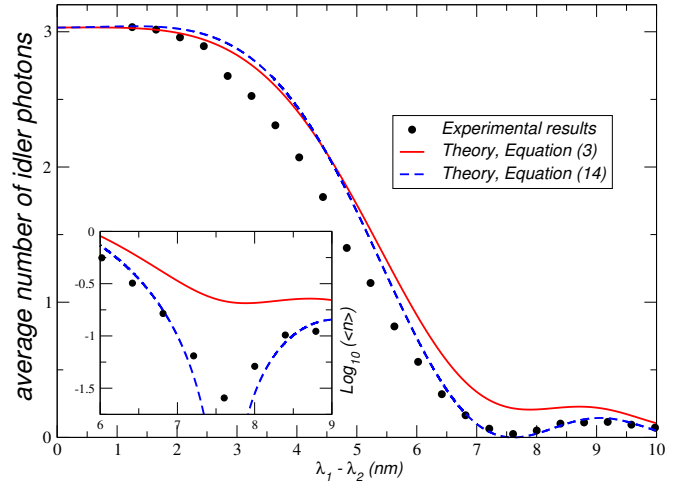


Fig. 3. Average number of photons per pulse of the idler wave as a function of wavelength separation between pump and signal fields. The circles represents the average of photons, the solid line represents the theoretical model given by (3) and the dashed line represents the theoretical model given by (14). We have used: $P_1(0) = 8.71$ mW, $P_2(0) = 1.62 \times 10^{-4}$ mW, and $\lambda_1 = 1547.57$ nm.

idler wave as a function of the spectral spacing between pump and signal fields. From Fig. 3 we can see that the theoretical model given by (14) describes better the experimental results than (3). However, in the region $2.8 \text{ nm} < \lambda_1 - \lambda_2 < 5 \text{ nm}$ the theoretical model and the experimental data does not coincide. That difference is analysed in section III-B.

B. Polarization effects

In the results presented in Fig. 3, we can see that with the increase of the spectral spacing between pump and signal fields, the average number of photons of the idler wave measured experimentally is smaller than the theoretical predictions. In the theoretical model presented in section III-A it was assumed that all fields remain co-polarized along the evolution in the fiber. However, when the spectral spacing between pump and signal is increased the fields go from an almost co-polarized situation to an decorrelated state of polarization (SOP), which leads to an loss of efficiency in the FWM process. That loss of efficiency can be seen as a reduction of the value of the nonlinear parameter γ [13], [14]. This can be described through a new parameter called effective nonlinear parameter γ_{eff} . If we replace the nonlinear parameter in (14) by the effective nonlinear parameter, γ_{eff} , the loss of efficiency in the generation of idler wave due to polarization effects can also be described by these two equations.

The variation of the effective nonlinear parameter is obtained by fitting the experimental data present in Fig. 3 to (14), with γ replaced by γ_{eff} . Results show, Fig. 3, that the γ_{eff} is approximately equals to γ for $\lambda_1 - \lambda_2 < 2.8$ nm. However, with the increasing separation between pump and signal fields, γ_{eff} decreases to $8\gamma/9$, and remains constant for $\lambda_1 - \lambda_2 > 5$ nm. This value for the γ_{eff} is in agreement with theoretical predictions for polarization dependent processes [13], [14]. In order to describe analytically the evolution of the γ_{eff} with

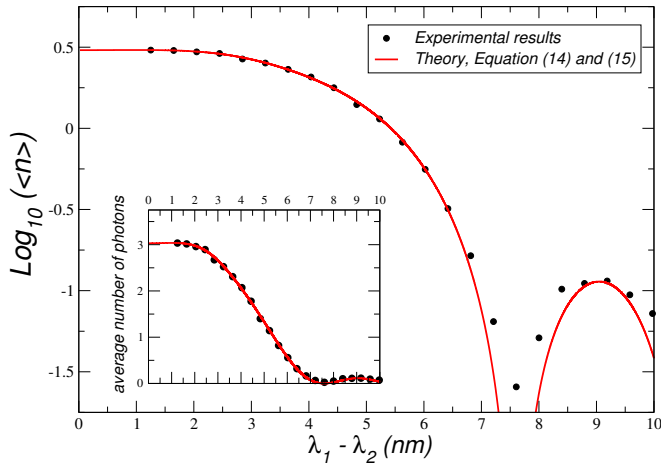


Fig. 4. Comparison between experimental data for the idler power and theoretical model, equation (14) with $\gamma_{eff}(\Delta\lambda)$ given by (15). The theoretical model and the experimental data shows good agreement. The experimental parameters used are the same as the ones used to obtain Fig. 3.

wavelength separation between pump and signal we represent that parameter with an hyperbolic secant function given by

$$\gamma_{eff}(\Delta\lambda) = \frac{8\gamma}{9} + \frac{\gamma}{9} \operatorname{sech}\left(\frac{(\Delta\lambda)^{A_0}}{T_0}\right), \quad (15)$$

where $A_0 \approx 2.36$ and $T_0 \approx 7.811 \times 10^{-21}$ are the fitting parameters.

Results presented in Fig. 3 show that until $\lambda_1 - \lambda_2 < 2.8$ nm the experimental data and theoretical prediction with $\gamma_{eff} = \gamma$ present a quasi perfectly match. That means that the fields remains co-polarized along the evolution in the fiber for small spectral spacings. According with the theory of the Principal States of Polarisation (PSP), exist a small frequency range over which the polarization mode dispersion vector is reasonably constant [15]

$$\Delta\omega_{psp} \approx \frac{\pi}{4\langle\Delta\tau\rangle}, \quad (16)$$

where $\langle\Delta\tau\rangle = 0.362$ ps is the mean differential group delay (DGD). The bandwidth range over which the SOP is reasonably constant is $\Delta\lambda_{psp} \simeq 2.75$ nm, which is in line with the value mentioned above, $\lambda_1 - \lambda_2 < 2.8$ nm. For $\lambda_1 - \lambda_2 > 5$ nm the experimental data is correctly describe with $\gamma_{eff} = 8\gamma/9$, which indicates that the pump and signal polarizations are mostly decorrelated.

Finally, in Fig. 4 we represent the measured optical power and the theoretical model for the idler wave as a function of spectral spacing between pump and signal fields. The results presented in Fig. 4 shows a completely agreement between the experimental data and the theoretical model given by (14) with $\gamma_{eff}(\Delta\lambda)$ given by (15).

IV. CONCLUSION

We implement a single photon-source based on the FWM process in optical fibers, capable to generate an average number of photons inferior to one, which has the advantage

of generate a variable average number of photons on the idler wave, by simple adjust of the wavelength separation between pump and signal fields. We investigated experimentally and theoretically the FWM process in a low power regime. We develop a theoretical model that governs the generation of the single-photons in the idler wave, for the case $P_1 \gg P_2$ with pump and signal powers maintained in a low power regime. We show that an accurate description of the generation of single-photons through FWM process can only be obtained by including the nonlinear contribution and polarization dependent effects in the scalar FWM theory. We also show experimentally that the randomly SOP variation in the fiber reduces the number of photons generated through the FWM process. We introduced the effective nonlinear parameter, $\gamma_{eff}(\Delta\lambda)$, and found that this parameter varies as an hyperbolic secant with the wavelength separation between pump and signal.

REFERENCES

- [1] G. P. Agrawal, *Nonlinear Fiber Optics*, 3rd ed. San Diego, California, USA: Academic Press, 2001.
- [2] R. H. Stolen, J. E. Bjorkholm, and A. Ashkin, "Phase-matched three-wave mixing in silica fiber optical waveguides," *Applied Physics Letters*, vol. 24, no. 7, pp. 308–310, 1974.
- [3] K. Inoue, "Four-wave mixing in an optical fiber in the zero-dispersion wavelength region," *J. Lightw. Technol.*, vol. 10, no. 11, pp. 1553–1561, 1992.
- [4] K. Washio, K. Inoue, and S. Kishida, "Efficient large-frequency-shifted three-wave mixing in low dispersion wavelength region in single-mode optical fiber," *Electronic Letters*, vol. 16, no. 17, pp. 658–660, 1980.
- [5] D. Bouwmeester, A. Ekert, and A. Zeilinger, *The Physics of Quantum Information*. Berlin: Springer-Verlag, 2000.
- [6] P. Antunes, P. S. André, and A. N. Pinto, "Single-photon source by means of four-wave mixing inside a dispersion-shifted optical fiber," in *FIO'06 - Frontiers in Optics*, USA, October 2006.
- [7] T. Jennewein, C. Simon, G. Weihs, H. Weinfurter, and A. Zeilinger, "Quantum cryptography with entangled photons," *Physical Review Letters*, vol. 84, no. 20, pp. 4729–4732, 2000.
- [8] id Quantique, "id 200 single-photon detector module," <http://www.idquantique.com/products/files/id200-operating.pdf>.
- [9] K. O. Hill, D. C. Johnson, B. S. Kawasaki, and R. I. MacDonald, "cw three-wave mixing in single-mode optical fibers," *J. Appl. Phys.*, vol. 49, no. 10, pp. 5098–5106, 1978.
- [10] N. Shibata, R. P. Braun, and R. G. Waarts, "Phase-mismatch dependence of efficiency of wave generation through four-wave mixing in a single-mode optical fiber," *IEEE J. Quantum Electron.*, vol. 23, no. 7, pp. 1205–1210, 1987.
- [11] J. R. Thompson and R. Roy, "Multiple four-wave mixing process in an optical fiber," *Optics Letters*, vol. 16, no. 8, pp. 557–559, 1991.
- [12] K. Kikuchi and C. Lorattanasane, "Design of highly efficient four-wave mixing devices using optical fibers," *IEEE Photon. Technol. Lett.*, vol. 6, no. 8, pp. 992–994, 1994.
- [13] P. K. Wai and C. R. Menyuk, "Polarization mode dispersion, decorrelation, and diffusion in optical fibers with randomly varying birefringence," *J. Lightw. Technol.*, vol. 14, no. 2, pp. 148–157, 1996.
- [14] Q. Lin and G. P. Agrawal, "Effects of polarization-mode dispersion on fiber-based parametric amplification and wavelength conversion," *Optics Letters*, vol. 29, no. 10, pp. 1114–1116, 2004.
- [15] C. D. Poole and R. E. Wagner, "Phenomenological approach to polarisation dispersion in long single-mode fibres," *Electronics Letters*, vol. 22, no. 19, pp. 1029–1030, 1986.